HEAT TRANSFER IN TRIANGULAR DUCTS WITH AXIAL CONDUCTION, CONTAINING POROUS MEDIUM

by

ABHISHEK BANERJEE

Presented to the Faculty of the Graduate School of

The University of Texas at Arlington in Partial Fulfillment

of the Requirements

for the Degree of

MASTER OF SCIENCE IN MECHANICAL ENGINEERING

THE UNIVERSITY OF TEXAS AT ARLINGTON

December 2011

ACKNOWLEDGEMENTS

I would like to thank my thesis advisor Dr.A.Haji Sheikh for his expert advice and for helping me through the challenging and tricky spots in my thesis. My sincere appreciation goes to Dr. Seiichi Nomura for helping me with the computations and for always being there to answer all my questions. I would also like to thank Dr. Dereje Agonafer for his valuable time to evaluate my thesis.

Finally I thank my parents, who have been a constant source of inspiration, all my friends and roommates for their support and encouragement throughout my Masters program.

November 10, 2011

ABSTRACT

HEAT TRANSFER IN TRIANGULAR DUCTS
WITH AXIAL CONDUCTION, CONTAINING
POROUS MEDIUM

Abhishek Banerjee, MS
The University of Texas at Arlington, 2011

Supervising Professor: A.Haji Sheikh

The objective of this study is to find a numerical solution for the velocity and temperature field in a duct of triangular cross-section area. A fully saturated porous medium is considered to be present in the duct. The study reports the contribution of axial conduction in heat transfer to flow passing through triangular porous passages. The terms in *x*-direction are retained in the energy equation due to the presence of axial conduction. Also, because of the geometrical asymmetry, non-orthogonal boundary conditions can exist and thus make the determination of heat transfer more difficult. The problem under consideration uses H2 boundary conditions namely locally constant wall heat flux circumferentially and in the axial direction as well. The placement of porous materials can enhance the transfer of heat to a flowing fluid.

The problem is divided into two parts. The first part deals with the finding the velocity field expression with the help of Brinkman's Momentum Equation. The second part uses the Energy

Equation for finding the temperature field. A fully developed flow is considered for the velocity field calculations and a thermally developing flow for the temperature calculations.

There are different methods for calculating the velocity field, one of them the method of Variational Calculus. The Variational Calculus leads to a minimization technique that provides a methodology known as the Galerkin method. Thus in the first phase, a weighted residual method (WRM) specifically the Galerkin method is used for calculations. This method allows using a polynomial function form known as basis function, which is finite, continuous and single valued.

Depending on the duct cross section, formation of the basis function under H2 boundary conditions needs special attention for triangular ducts. The calculations for the temperature field might be formidable. Thus a Mathematica program is used for calculating the eigenvalues and eigenfunctions and for calculating various parameters such as Nusselt Number (Nu) and the heat transfer coefficient. The Mathematica program is as shown in Appendix A.

TABLE OF CONTENTS

LIST OF ILLUSTRATIONS

Figure Page

LIST OF TABLES

NOMENCLATURE

A_m, B_m =coefficient in a series

A = Cross-Section area

P=Perimeter

C= ρ* C_p

C_p = specific heat

Da = Darcy number (K/H^2)

K= permeability coefficient

k = Thermal conductivity

H = Height of the isosceles triangle

W = half the base of isosceles triangle

L_c = characteristic length

m,n= indices

i, j = indices

f_j = basis functions in weighted residual method

N=Number of terms in series

D_h = hydraulic diameter (4A/P)

Nu_d= Nusselt Number (hD_h/k)

T_w = wall temperature when x>0

T_b = bulk temperature

u = velocity

U= average velocity

p= Pressure

Pe= Peclet Number (UL/α)

Pr= Prandtl Number ($\mu C_p/k$)

WRM=Weighted Residual method

$\hat{x}$ = axial coordinate

$x = (\hat{x}/W)/Pe$

$y, z = \hat{y}/W \quad and \quad \hat{z}/W$

y, z = coordinates

q_w = wall heat flux

T= Total Temperature

T_i = wall temperature when x<0

Greek symbols

α = Thermal diffusivity

β_n , λ_m = eigenvalues

θ= dimensionless temperature

μ = viscosity coefficient

ρ= density

Φ_m , Ψ_m = Eigenfunctions

ϕ = constant pressure gradient

Subscripts

w for wall

1 for x<0

2 for x>0

CHAPTER 1

INTRODUCTION

Laminar flow and heat transfer inside ducts has been a subject of interest for several decades. The Laminar convective heat transfer rate in ducts of different shaped boundaries is important for the proper design of compact heat exchangers and other heat transfer equipment such as boilers, industrial furnaces, combustors and rocket engines etc. In many cases, it is required to use a heat exchanger with a very high ratio of heat transfer area as related to overall volume. So, a heat exchanger with a triangular cross section is a good option due to its excellent compactness and cost effectiveness as compared to traditional shell and tube heat exchanger. Another advantage of this geometry is that it is easy to construct with very thin materials and the strength is rather high even with very thin foils.

1.1 Literature Review

There has been a lot of analytical and numerical research on heat transfer through different cross section area ducts. Different methods have been used to analyze the modes of heat transfer. Sparrow and Siegel [1] studied the variations of the heat transfer coefficient for rectangular ducts. An analytical method for the numerical calculation of the heat transfer coefficient in arbitrarily shaped ducts with constant wall temperature at the boundary is presented in [2] wherein the flow is considered to be laminar and fully developed. The method presented in [2] makes use of Galerkin-type technique for computation of the temperature and the Nusselt number. This method is applied to circular pipes and ducts with rectangular, isosceles, triangular, and right triangular cross sections. The heat transfer in the entrance region is investigated using extended Graetz problem [3], which takes into account

axial conduction in the fluid. It shows various approximate methods for calculation of eigenvalues and eigenfunctions for laminar and turbulent flow. Shah [4] explained the least square matching technique to analyze fully developed laminar fluid flow and heat transfer in ducts of an arbitrary cross-section. As an application of the method, he presented the results for the geometries of isosceles triangular, rounded corner equilateral triangular, rhombic, and trapezoidal cross-sections. A similar work on isosceles and right triangular ducts was performed by Lakshminarayanan and Haji Sheikh [5].Galerkin method was used to compute the velocity field and a Green's Function method for the energy equation.

The particular topic of thermally developing forced convection in porous media is surveyed by Nield and Kuznetsov [6].Recent papers involving porous-media forced convection in ducts of various shapes include those by Haji-Sheikh and Vafai [7] and Hooman and coworkers [8-10].A similar analysis on the circular ducts was performed by Haji-Sheikh et al.[11].The extended weight residual method described in [12-13], is employed in order to determine the temperature distribution from the energy equation. Following the computation of temperature field, expressions are present for local Nusselt number and bulk temperature. We can observe that ducts filled with porous models enhance the heat transfer.

The axial conduction is expected to have a strong effect on the heat transfer to flow through various passages near the entrance region, depending on the size of Peclet number. When the Peclet number becomes small, the contribution of axial conduction becomes significant. Using separation of variables, a mathematical procedure that includes the contribution of axial conduction is illustrated by Lahjomri and Oubarra [14].The axial conduction has a significant effect in fluid saturated porous passages and the Graetz-type solutions are in [15] for parallel plate and circular ducts. The method of variational calculus is used for calculation of velocity field in [16].The minimization process using the variational calculus is called the weighted residual method (WRM).

Thus we observe that the axial conduction is usually ignored when dealing with the porous media, for the purpose of easier calculations. As seen in [5] the boundary conditions of the first kind are considered and axial conduction, viscous dissipation are neglected .This paper talks about triangular ducts with H2 boundary conditions and retaining the axial conduction terms in the energy equation.

The main reason for using Galerkin method over Graetz solution is that for a flow in a two dimensional velocity field, the solution is not separable which makes the method of weighted residuals a desired choice. The Galerkin method provides a straightforward approach to the solution of boundary value problems. Therefore instead of developing the functional, one can directly apply the Galerkin method to the boundary value problem. The Galerkin method basically involves expressing the given boundary value problem in terms of a standard mathematical relation, generating a set of complete and continuous base functions, formulating the matrix, and determining the solution.

In Chapter 2, all the mathematical equations as well as assumptions used for computations of velocity and temperature field are discussed. The step by step procedure to obtain the velocity field and the transformation required for temperature field are explained. A process to calculate the eigenvalues is also displayed.

In Chapter 3, all the results obtained by applying the equations from Chapter 2 are presented and changes in wall temperature, bulk temperature and Nusselt number are observed as the flow progresses along the axial direction. The temperature field is also seen to be changing with increasing values of the z-coordinate showing the continuous changing nature of the temperature field.

Chapter 4 talks about all the conclusions drawn from results and graphs plotted in the previous chapter and suggestions for future work are drawn.

1.2 Research Objectives

The main objective of this thesis is to numerically determine the temperature and velocity fields for triangular ducts considering H2 boundary conditions that include the effects of axial conduction. This paper focuses on triangular ducts .The method of weighted residuals is used for velocity calculations and the evaluation of the energy equation using the Mathematica program developed for the case in consideration. It gives the values of eigenvalues and eigenvectors for the determination of temperature field and heat transfer coefficient.

The basic governing equations for determining the velocity field and temperature field of the porous medium considering hydrodynamically fully developed flow are given by the Brinkman momentum equation and the energy equation.

CHAPTER 2

ANALYSIS AND ASSUMPTIONS

(MATHEMATICAL MODEL)

This chapter presents the mathematical model of the problem in consideration. The Momentum Equation is used for development of the velocity field. The Momentum Equation for flow over porous media is to be modified. In this application there will be an additional internal force per unit volume, F_i ,within the material element, due to the drag force as flow passes over solid particles; for the Brinkman model $F_i = \mu V / K$. The parameter *K*, called the permeability, depends on the material porosity ε= (volume) $_{fluid}$ / (volume) $_{solid+fluid}$. In this study, the flow is hydrodynamically fully developed and velocity depends on y and z coordinates. A standard Galerkin method is used for computations of the velocity field. For a fluid passage with constant but arbitrary cross section the Brinkman momentum equation,

$$\mu_e \left(\frac{\partial^2 u}{\partial \hat{y}^2} + \frac{\partial^2 u}{\partial \hat{z}^2} \right) - \frac{\mu}{K} u - \frac{\partial p}{\partial \hat{x}} = 0$$

leads towards the computation of a fully developed velocity profile in which the pressure gradient $\emptyset = -\partial p / \partial x$ is a constant.

2.1 Velocity Field

The Momentum equation is used for development of the velocity field. Henry Darcy, through experiments has determined the proportionality between flow rate and applied pressure difference for steady-state, unidirectional flow through porous medium; expressed it by equation

$$\frac{\partial p}{\partial \hat{x}} = -\frac{\mu}{K} u \tag{2.1}$$

Darcy's equation is extended by Brinkman's Momentum equation, which includes the medium's porosity

$$\frac{\partial p}{\partial \hat{x}} = -\frac{\mu}{K} u + \mu_e \left(\frac{\partial^2 u}{\partial \hat{y}^2} + \frac{\partial^2 u}{\partial \hat{z}^2} \right) \tag{2.2}$$

where

μ= Fluid viscosity

μ_e= effective viscosity

Under a hydrodynamically fully developed condition,

$\phi = -\frac{\partial p}{\partial x}$ (Constant pressure gradient)

The non dimensional form of the Eqn. 2.2 can be expressed as

$$\left(\frac{\partial^2 \overline{u}}{\partial y^2} + \frac{\partial^2 \overline{u}}{\partial z^2} \right) - \frac{1}{MDa} \overline{u} + 1 = 0 \tag{2.3}$$

Wherein $y = \hat{y}/L_c$, $z = \hat{z}/L_c$, $M=\mu_e/\mu$, $\overline{u} = \mu_e u/(\emptyset L_c^2)$ and $Da = K/L_c^2$ is the Darcy number. Moreover, μ_e is the effective fluid viscosity, μ is the fluid viscosity, K is the permeability and L_c is arbitrarily chosen as the characteristic length. M changes in value depending on the particles in flow but overall varies as a parameter MDa. As can be demonstrated by Lundgren [17], the ratio of M is in the range of 0.28-1.

Computation of the velocity field is performed using Galerkin Based Integral method that uses a set of basis functions, which are finite, single valued and continuous in the area of cross section

of the flow , in the duct. A polynomial form basis function gives a closed form solution to the problem.

Using the computed velocity, the mean velocity of the duct is given by

$$U_{avg} = \frac{1}{A}\int_A u \, dy \tag{2.4}$$

For an isosceles triangular duct, Fig 2.1, the velocity is considered have the form

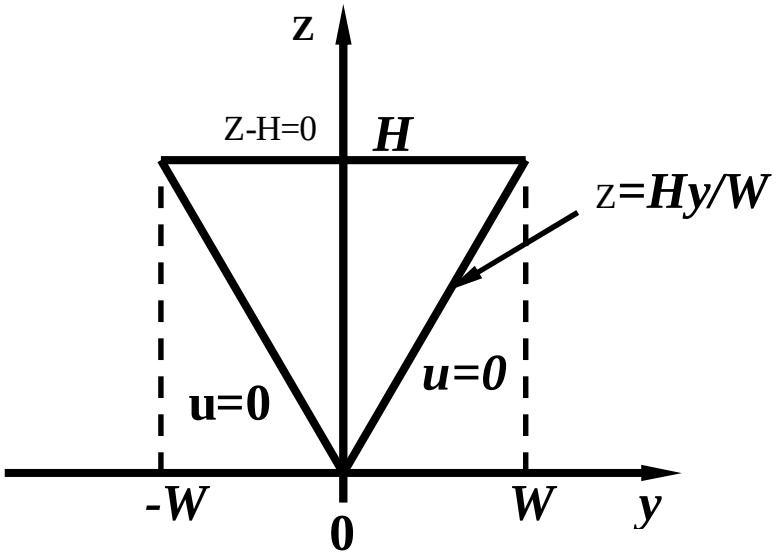

Figure 2.1 The triangular cross section duct with major dimensions

$$\bar{u}(y,z) = \sum_{j=1}^{N} \delta_j \eta_j(\hat{y},\hat{z}) \tag{2.5}$$

Where the basis functions are

$$\eta_j = [\hat{z}^{\,2} - (h\,y/w)^{\,2}]^* (\hat{z} - h)^* \hat{z}^{\,q-1} * \hat{y}^{\,2j-2} \tag{2.5.2}$$

In the Brinkman's Momentum equation, Eqn.2.3 velocity $\bar{u}$ is substituted by the basis function relation as shown above in Eqn.2.5 and solved by using the Galerkin method, that is, both sides of Eqn.2.3 are multiplied by η_i dA and integrated over area A.

$$\int_0^w \int_{y/w}^H \eta_i \left(\left(\frac{\partial^2 \bar{u}}{\partial y^2} + \frac{\partial^2 \bar{u}}{\partial z^2} \right) - \frac{1}{MDa} \bar{u} \right) dA + \int_o^w \int_{y/w}^H \eta_i dA = 0 \tag{2.6}$$

We then use the standard Galerkin method to solve the above integral leading to the matrix form

$$E.\Delta = \Omega \tag{2.7}$$

where the matrix E has the elements

$$e_{ij} = \int_A \left[\nabla^2 \eta_j(y,z) - \eta_j / MDa \right] \eta_i(\hat{y},\hat{z}) \, \mathrm{dA} \tag{2.8}$$

and the vector Ω has elements

$$\omega_i = -\int_A \eta_i(y,z) dA \tag{2.9}$$

Following the inversion of matrix Ω, the unknowns (δ_1, δ_2… δ_n) are the elements of the vector

$$\Delta = E^{-1}.\Omega \tag{2.10}$$

2.2 Temperature Field

Temperature distribution field can be obtained from energy equation provided the local thermal equilibrium exists. The energy equation can be stated as

$$\rho C_p \frac{DT}{Dt} + \nabla . \overset{\rho}{q} - q_r = -p\nabla V + \mu\phi \tag{2.11}$$

where

q_r = volumetric heat generation; can be neglected.

$\mu\phi$ = viscous dissipation is to be neglected in this study.

$p\nabla V$ = reversible work to be neglected because the flow is an incompressible flow.

ρ = Fluid density.

$\overset{\upsilon}{q}$ = Heat flux vector in accordance with Fourier's law of conduction.

$$\overset{\upsilon}{q} = -k\nabla T = -k\left(\frac{\partial T}{\partial \hat{x}} i + \frac{\partial T}{\partial \hat{y}} j + \frac{\partial T}{\partial \hat{z}} k\right) \tag{2.12}$$

Substituting for $\overset{\upsilon}{q}$ and neglecting insignificant terms Eqn.2.11 becomes

$$\rho C_p \left(\frac{\partial T}{\partial t} + u\frac{\partial T}{\partial \hat{x}} + v\frac{\partial T}{\partial \hat{y}} + w\frac{\partial T}{\partial \hat{z}}\right) - k\left(\frac{\partial^2 T}{\partial \hat{x}^2} + \frac{\partial^2 T}{\partial \hat{y}^2} + \frac{\partial^2 T}{\partial \hat{z}^2}\right) = 0 \tag{2.13}$$

Furthermore, the quantities $\frac{\partial T}{\partial t}, v\frac{\partial T}{\partial \hat{y}}, w\frac{\partial T}{\partial \hat{z}}$ have zero values for steady state condition and unidirectional flow. Thus, the steady state thermal energy equation becomes

$$\rho C_p u \frac{\partial T}{\partial \hat{x}} = k\left(\frac{\partial^2 T}{\partial \hat{x}^2} + \frac{\partial^2 T}{\partial \hat{y}^2} + \frac{\partial^2 T}{\partial \hat{z}^2}\right) \tag{2.14}$$

subject to the boundary conditions

$$\left(\frac{\partial T}{\partial n}\right)_{wall} = \begin{cases} 0 & when \quad \hat{x} < 0 \\ q_w / k & when \quad \hat{x} \geq 0 \end{cases} \tag{2.15}$$

$T=T_i$ as $\hat{x} \rightarrow -\infty$ (2.15a)

$\left(\frac{\partial T}{\partial \hat{x}}\right)$ = finite as $\hat{x} \rightarrow \infty$ (2.15b)

The last condition implies that the slope of the temperature function has a finite value as x approaches infinity. The parameter q_w is the wall heat flux (per unit area) entering the fluid passage between x=0 and x=∞.Using the characteristic length L_c = W and simplifying, the energy equation given by Eqn.2.14, it becomes

$$\frac{\partial^2 T}{\partial y^2} + \frac{\partial^2 T}{\partial z^2} = \frac{u}{U}\frac{\partial T}{\partial x} - \frac{1}{Pe^2}\frac{\partial^2 T}{\partial x^2} \tag{2.16}$$

where

$y = \hat{y}/W$, $z = \hat{z}/W$, $x = (\hat{x}/W)/Pe$ and Pe = ρC_p W U/k

The computational procedure for the temperature field requires some modifications mainly for selection of basis functions and determination of the transformation function. This applies to the problem, when the boundary conditions of the second kind are given in the y and z directions. One of the ways to accommodate the locally constant heat flux is to use a temperature

transformation in the dimensionless form of the energy equation. This transformation removes the non-homogeneity in the boundary condition of the second kind.

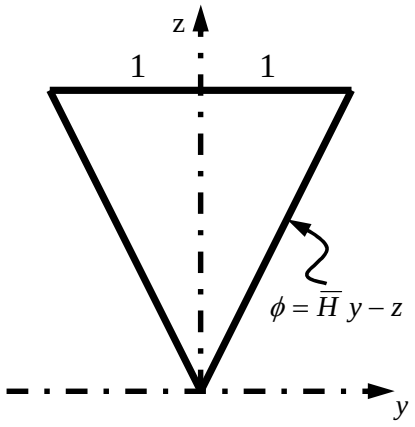

Figure 2.2 The isosceles triangular duct in dimensionless space

To accomplish this task, let

$$\phi = \bar{H}y - z \tag{2.17}$$

where $\bar{H}$ =*H*/w

The unit normal $\underset{\rho}{h}$ has the magnitude of 1.Therfore the expression for $\underset{\rho}{h}$ is

$$\underset{\rho}{h} = \frac{\bar{H}}{\sqrt{1+\bar{H}^2}}\underset{\rho}{i} - \frac{1}{\sqrt{1+\bar{H}^2}}\underset{\rho}{j} \tag{2.18}$$

and select a complimentary solution such as

$$\theta_c = ay^2 + bz + cz^2 \tag{2.19}$$

so that the $\nabla\theta_c \cdot \underset{\rho}{h} = 1$ everywhere on the contour of the duct. After performing necessary operations of Eqn.2.19 and Eqn.2.18 to substitute in the above expression, we get the following values

$$\left.\frac{\partial \theta_c}{\partial \bar{z}}\right|_{\phi=0} = \left[\frac{2ay\bar{H}}{\sqrt{1+\bar{H}^2}} - \frac{b}{\sqrt{1+\bar{H}^2}} - \frac{2cz}{\sqrt{1+\bar{H}^2}}\right]_{z=\bar{H}y}$$
$$= \frac{2ay\bar{H}}{\sqrt{1+\bar{H}^2}} - \frac{b}{\sqrt{1+\bar{H}^2}} - \frac{2cy\bar{H}}{\sqrt{1+\bar{H}^2}} = 1 \qquad (2.20)$$

This requires having $c = a$ and $b = -\sqrt{1+\bar{H}^2}$. The condition at $z = \bar{H}$ leads to the relation

$$\left.\frac{\partial \theta_c}{\partial z}\right|_{z=h} = (b + 2cz)\Big|_{z=\bar{H}} = b + 2c\bar{H} = 1 \qquad (2.21)$$

Solving the above equation leads to the relation $c = (1-b)/(2\bar{H})$ that gives

$$a = c = \frac{1+\sqrt{1+\bar{H}^2}}{2\bar{H}}$$

and then substituting the constants a, b, c in Eq.2.19 we get

$$\theta_c = \frac{1+\sqrt{1+\bar{H}^2}}{2\bar{H}}\left(y^2 + z^2\right) - \sqrt{1+\bar{H}^2}\; z \qquad (2.22)$$

The temperature solution of Eqn.2.16 is deterministic if one defines the function $\theta_1(x, y, z)$ such that

$$T - T_i = \left(\frac{q_w W}{k}\right)\theta_1(x, y, z) \qquad (2.23)$$

when x< 0. Also a function $\theta_2(x, y, z)$ is defined so that

$$T - T_i = \left(\frac{q_w W}{k}\right)\left[\theta_2(x,y,z) + \theta_c + \omega(y,z)\right] \qquad (2.23\ a)$$

After the replacement of θ_c, the solution becomes

$$\text{i.e. } T - T_i = \left(\frac{q_w W}{k}\right)\left[\theta_2(x,y,z) + c_0 x + \frac{1+\sqrt{1+\overline{H}^2}}{2\overline{H}}(y^2+z^2) - \sqrt{1+\overline{H}^2}\,z \right. \qquad (2.24)$$

$$\left. + \omega(y,z)\ \right]$$

when x>0. The function θ_c is the complementary solution as shown in Eq.2.22 and as we can see from Eqn.2.24, the terms in the expression do not go to zero after double differentiation. This introduces a constant that would behave as a volumetric heat source. Thus a function $\omega(y,z)$ is added to make the partial differential equation homogenous by eliminating the volumetric heat flux term which is $\nabla^2\theta_c$.

After substituting Eqn.2.24 in Eqn.2.16 for the temperature solution, a properly selected function $\omega(y,z)$ is a transformation that satisfies the relation

$$\frac{\partial^2\omega}{\partial y^2} + \frac{\partial^2\omega}{\partial z^2} = c_0 - \nabla^2\theta_c \qquad (2.25)$$

where c_0 is an arbitrary constant and can be chosen as required. The value of c_0 in this equation can be arbitrarily taken as below and the value of $\nabla^2\theta_c$ can be taken from Eqn.2.22 as follows

$$c_0 = \frac{4}{D_h}\frac{u}{U} \tag{2.25a}$$

$$\nabla^2\theta_c = \frac{2}{H}\left(1+\sqrt{1+H^2}\right) \tag{2.25b}$$

where

$$D_h = 4\mathrm{A/P} = \left(\frac{H*W}{2(W+\sqrt{H^2+W^2}}\right)*4 \tag{2.26}$$

Now applying the above values in Eqn.2.25 we get

$$\frac{\partial^2\omega}{\partial y^2}+\frac{\partial^2\omega}{\partial z^2} = \left(\frac{2}{H}\left(1+\sqrt{1+H^2}\right)\right)\left(\frac{u}{U}-1\right) \tag{2.27}$$

that satisfies the homogenous boundary condition.

$$\frac{\partial\omega}{\partial y} = 0 \quad at \qquad z = \pm\overline{H}$$

$$\frac{\partial\omega}{\partial z} = 0 \quad at \qquad z = \pm Hy/w \tag{2.28}$$

A simple Galerkin method can be used for the computation of $\omega(y,z)$. After substitution of Eqn.2.24 into Eqn.2.16, for $\theta_2(x,y,z)$ to be homogenous at boundaries, the following condition is to be satisfied

$$\frac{\partial^2\omega}{\partial y^2}+\frac{\partial^2\omega}{\partial z^2} = \frac{4u}{D_h U}-\nabla^2\theta_c \tag{2.28 a}$$

Now $\omega(y,z)$ can be written as

$$\omega(y,z) = \sum_{j=1}^{N} e_j f_j(y,z) \tag{2.29}$$

where f_j is a set of basis functions and e_j are the required coefficients. Now substituting the value of $\omega(y,z)$ from Eqn.2.29 back into Eqn.2.28a we get

$$\sum_{j=1}^{N} e_j \int_A f_i \nabla^2 f_j \, dA = \int_A \left(\frac{4}{D_h} \frac{u}{U} - \nabla^2 \theta_c \right) f_i \, dA \qquad (2.29\text{ a})$$

The above equation can be expressed as

$$A.D = F \qquad (2.29\text{ b})$$

where A is a matrix which has elements

$$a_{ij} = \int_A f_i \nabla^2 f_j \, dA \qquad (2.30)$$

and the vector F has the elements

$$\varepsilon_i = \int_A \left(\frac{4}{D_h} \frac{u}{U} - \nabla^2 \theta_c \right) dA \qquad (2.31)$$

After the matrix inversion the computed values of e_j in vector D are substituted back into Eqn.2.29b for finding $\omega(y,z)$.

Therefore, both the $\theta_1(y, z)$ and $\theta_2(y, z)$ functions must also satisfy the homogenous boundary conditions of the second kind at z= $\overline{H}$ and z = $\overline{H}y$. Substituting these dimensionless parameters in Eq.2.16, the energy equation in dimensionless form becomes

$$\frac{\partial^2 \theta_1}{\partial y^2} + \frac{\partial^2 \theta_1}{\partial z^2} = \frac{u}{U} \frac{\partial \theta_1}{\partial x} - \frac{1}{Pe^2} \frac{\partial^2 \theta_1}{\partial x^2} \qquad (2.32\text{ a})$$

$$\frac{\partial \theta_1}{\partial y} = 0 \quad at \quad \bar{z} = \overline{H}$$

$$\frac{\partial \theta_1}{\partial z} = 0 \quad at \quad \bar{z} = \pm \overline{H}y \qquad (2.32\text{ b})$$

Also the functional form of Eqn.2.24 is selected so that $\theta_2(y, z)$ satisfies a similar partial differential equation; that is

$$\frac{\partial^2\theta_2}{\partial y^2} + \frac{\partial^2\theta_2}{\partial z^2} = \frac{u}{U}\frac{\partial\theta_2}{\partial x} - \frac{1}{Pe^2}\frac{\partial^2\theta_2}{\partial x^2} \qquad (2.33\ a)$$

$$\frac{\partial\theta_2}{\partial y} = 0 \quad at \quad \bar{z} = \overline{H}$$

$$\frac{\partial\theta_2}{\partial z} = 0 \quad at \quad \bar{z} = \pm\overline{H}y \qquad (2.33\ b)$$

Thus both Eqn.2.32 (a) and 2.33(a) have homogenous boundary conditions along the contour of the triangular duct. Then the solutions for $\theta_1(x, y, z)$ and $\theta_2(x, y, z)$ functions have the form

$$\Theta_1(x, y, z) = \sum_{m=0}^{\infty} A_m\phi_m(y, z)e^{\beta_m x} \quad when \quad x \le 0 \qquad (2.34)$$

$$\Theta_2(x, y, z) = \sum_{m=0}^{\infty} B_m\psi_m(y, z)e^{-\lambda_m x} \quad when \quad x \ge 0 \qquad (2.35)$$

The calculation of eigenfunctions ϕ_m and ψ_m takes place at a later stage. The two sets of axial eigenvalues, β_m and λ_m , for insertion into Eqn.2.34 and 2.35 must be positive in order to satisfy the conditions when $x \to -\infty$ and $x \to +\infty$, respectively. For determination of $\theta_1(x, y, z)$, the eigenvalue β_0 has no contribution since the condition

$\theta_1(-\infty, y, z) = 0$ makes $A_0 = 0$ .The solution of $\theta_2(x, y, z)$ includes the contribution of $\lambda_0 = 0$ when m=0.

Next, the compatibility conditions at x=0 are to be used for determination of A_m and B_m coefficients. The first compatibility conditions is $T_1 (0-, y, z) = T_2 (0+, y, z)$ and Eqs.2.23 and 2.24 gives the relation

$\Theta_1 (x, y, z) = \theta_2(x, y, z) + F(y, z)$ (2.36 a)

wherein

$$F(y, z) = \theta_c + \omega(y, z) \tag{2.36 b}$$

The use of the second compatibility condition $[\partial T/\partial x]_{x=0-} = [\partial T/\partial x]_{x=0+}$ results in the relation

$$\left[\frac{\partial \theta_1(x, y, z)}{\partial x}\right]_{x=0} = \left[\frac{\partial \theta_2(x, y, z)}{\partial x}\right]_{x=0} + c_0 \tag{2.37}$$

Wherein $c_0 = \frac{4}{D_h}\frac{u}{U}$

Now the final temperature solutions for these fluid passages require the determination of the coefficients A_m and B_m in Eqs.2.34 and 2.35.To accomplish this task the orthogonality condition as given in [16, Eqn. 21] can be used to give

$$\int_A \left(\frac{u}{U} + \frac{\beta_m + \beta_n}{Pe^2}\right)\phi_m \phi_n dA = \begin{cases} 0 & when \quad \beta_m \neq \beta_n \\ N_m & when \quad \beta_m = \beta_n \end{cases} \tag{2.38a}$$

and

$$\int_A \left(\frac{u}{U} + \frac{\lambda_m + \lambda_n}{Pe^2}\right)\psi_m \psi_n dA = \begin{cases} 0 & when \quad \lambda_m \neq \lambda_n \\ N_m & when \quad \lambda_m = \lambda_n \end{cases} \tag{2.38b}$$

These two solutions are different and they are presented separately.

The substitution of θ_1 and θ_2 functions from Eqn.2.34 and 2.35 into Eqn.2.36 and Eqn.2.37 would lead to the following two relations for determination of coefficient A_m and B_m,

$$\sum_{m=1}^{\infty} A_m \phi_m(y, z) = \sum_{m=1}^{\infty} B_m \psi_m(y, z) + F(y, z) \tag{2.39a}$$

and

$$\sum_{m=1}^{\infty} A_m \beta_m \phi_m(y,z) = \sum_{m=1}^{\infty} B_m \lambda_m \psi_m(y,z) + c \qquad (2.39b)$$

After multiplying both sides of Eqn. (2.39a) by $\beta_n / Pe^2 - u / U$ and both sides of Eqn. (2.39b) by $1/Pe^2$ and then adding the resulting relations to get

$$\sum_{m=1}^{\infty} A_m \left(\frac{\beta_m + \beta_n}{Pe^2} - \frac{u}{U} \right) \phi_m(y,z) = \sum_{m=1}^{\infty} B_m \left(\frac{-\lambda_m + \beta_n}{Pe^2} - \frac{u}{U} \right) \psi_m(y,z) + \frac{c}{Pe^2} + F(y,z) \left(\frac{\beta_n}{Pe^2} - \frac{u}{U} \right) \qquad (2.40)$$

To apply the orthogonality condition, multiply both sides of Eqn.2.40 by $\Phi_n(y, z)dA$ for a given index n and then integrate over the duct's cross section area, A to give the relation

$$\sum_{m=1}^{\infty} A_m \int_A \left(\frac{\beta_m + \beta_n}{Pe^2} - \frac{u}{U} \right) \phi_m(y,z) \phi_n(y,z) dA = \sum_{m=1}^{\infty} B_m \int_A \left(\frac{-\lambda_m + \beta_n}{Pe^2} - \frac{u}{U} \right) \psi_m(y,z) \phi_n(y,z) dA + \int_A \left[\frac{c}{Pe^2} + F(y,z) \left(\frac{\beta_n}{Pe^2} - \frac{u}{U} \right) \right] \phi_n(y,z) dA \qquad (2.41)$$

According to the orthogonality condition, Eqn.2.38b, the first term on the right side of Eqn.2.41 would vanish since $-\beta_n \neq \lambda_m$ as they are in different domains for the same eigenfunctions. Therefore the non-zero terms when $\beta_n = \beta_m$ for m = n lead to the value of

$$A_n = \frac{\int_A \left[\frac{c}{Pe^2} + F(y,z) \left(\frac{\beta_n}{Pe^2} - \frac{u}{U} \right) \right] \phi_n(y,z) dA}{\int_A \left(\frac{2\beta_n}{Pe^2} - \frac{u}{U} \right) \phi_n^2(y,z) dA} \qquad for \quad n = 1,2,3... \qquad (2.42)$$

for insertion in Eqn.2.34, when x<0. A similar procedure is repeated for determination of the B_n in Eqn.2.35. After multiplying both sides of Eqn.2.38a by $-\lambda_n/Pe^2 - u/U$ and both sides of Eqn.2.38b by $1/Pe^2$ and then adding the resulting expressions yields the equation

$$\sum_{m=1}^{\infty} A_m \left(\frac{\beta_m - \lambda_n}{Pe^2} - \frac{u}{U} \right) \phi_m(y,z) \psi_n(y,z) dA = -\sum_{m=1}^{\infty} B_m \left(\frac{-\lambda_m - \lambda_n}{Pe^2} - \frac{u}{U} \right) \phi_m(y,z) \qquad (2.43)$$

$$\frac{c}{Pe^2} + F(y,z) \left(\frac{-\lambda_n}{Pe^2} - \frac{u}{U} \right)$$

Next multiply both sides of Eqn.2.43 by ϕ_n (y, z) dA and integrating the resulting result over the cross section area A yields

$$B_n = \frac{\int_A \left[\frac{c}{Pe^2} - F(y,z) \left(\frac{\lambda_n}{Pe^2} + \frac{u}{U} \right) \right] \psi_n(y,z) dA}{\int_A \left(\frac{2\lambda_n^2}{Pe^2} + \frac{u}{U} \right) \psi_n^2(y,z) dA} \qquad for \quad n = 1,2,3... \qquad (2.44)$$

for determination of θ_1 when x<0 following insertion in Eqn.2.35.

Now after the calculation of the coefficients A_n and B_n they can be substituted back into Eqn.2.34 and 2.35 for getting the temperature solution.

The next step of the calculation is to find the eigenfunctions which will give us the homogenous solutions θ_1 and θ_2 at the boundary. ψ_m, which is a linear combination of a set of linearly independent basis functions, can be written as

$$\psi_m(y,z) = \sum_{j=1}^{N} d_{mj} f_j(y,z) \quad \text{when } x \geq 0 \qquad (2.45\ a)$$

$$\phi_m(y,z) = \sum_{j=1}^{N} d_{mj} f_j(y,z) \quad \text{when } x < 0 \qquad (2.45\ b)$$

The basis functions are generated using the Mathematica program and are used in the above equation. The basis functions f_j(y, z) are selected so that they satisfy the same type of homogenous boundary conditions as those for θ_1 and θ_2, along the boundary of the duct.

Now the numerical computation begins by finding the elements of the matrices A, B and C as given below

$$a_{ij} = \iint_A f_i(y,z)\nabla^2 f_j(y,z)dA \tag{2.46a}$$

$$b_{ij} = \iint_A \left(\frac{u}{U}\right) f_i(y,z)\, f_j(y,z)dA \tag{2.46b}$$

$$c_{ij} = \iint_A \frac{1}{Pe^2}\, f_i(y,z)\, f_j(y,z)dA \tag{2.46c}$$

wherein parameter A represents the cross section area in dimensionless space. Then the eigenvalues and eigenvectors are obtainable from the equation

$$(A+\lambda B+\lambda^2 C)\, d = 0 \tag{2.47}$$

Next, this can be reduced to a classical eigenvalues problem [18] by using the vectors v and w defined as $w = \lambda d = \lambda v$. After appropriate substitutions, this leads to the eigenvalue problem;

$$\begin{bmatrix} 0 & I \\ A & B \end{bmatrix}\begin{bmatrix} v \\ w \end{bmatrix} - \lambda \begin{bmatrix} I & 0 \\ 0 & -C \end{bmatrix}\begin{bmatrix} v \\ w \end{bmatrix} = 0 \tag{2.48}$$

This leads to two sets of eigenvalues, a positive set and a negative set. Standard computational packages are available for determination of these eigenvalues designated as λ_m. For each eigenvalue, λ_m, there is a set of related coefficients d_{mj} which are the members of eigenvectors d_m. The computed eigenvalues, λ_m are expected to be real but they can be positive or negative. The eigenvalues in Eqn.2.47 and the corresponding eigenvector coefficients in Eqn.2.45 are computed using the computer package Mathematica.

CHAPTER 3

RESULTS AND DISCUSSIONS

The detailed procedure explained in the previous chapters is employed to get the final temperature and velocity fields. The double integrations and matrix inversions have been solved by using mathematical software, namely Mathematica. It is observed that the convergence of the solution increases as the order of the polynomial increases. In other words, the accuracy of the solution increases at x=0 for higher order of basis functions and more number of eigenvalues used. Below listed are the plots for the various parameters

3.1 Nusselt number vs. Axial coordinate

Using the computational procedure mentioned in Chapter 2 the Nu_d values are presented for different values of MDa and for Pe=1, 2, 5, 10, 50. The upper and lower bounds of the graphs are taken at MDa=0 and MDa= ∞, which represent slug flow and free flow respectively. A log-log scale has been selected for the x and y axis to see the pattern in which the Nusselt number behaves. There is an increase in the Nusselt number as the Peclet number is increased in each of the graphs. There is an upward shift in the Nusselt number as the Peclet number of the flow increases.

The graphs are shown below in this section as follows.

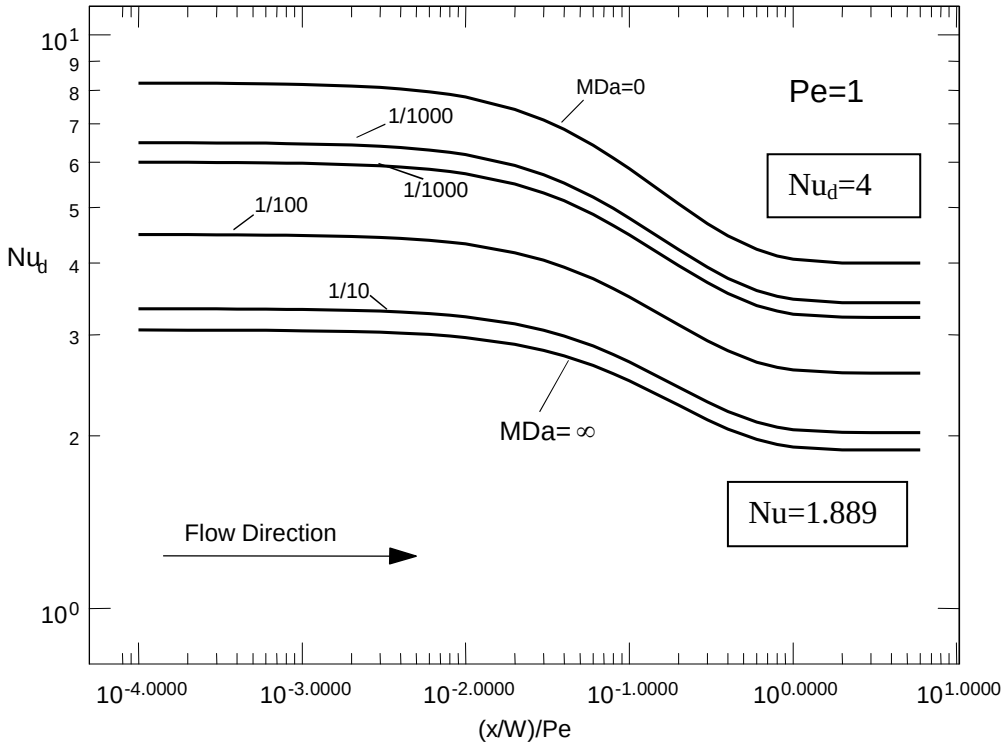

Figure 3.1 Computed Nu_d as a function of dimensionless axial coordinate for Pe=1.The values displayed on the right hand side of the figure are the fully developed values (attained asymptotically as $x \rightarrow \infty$) for the limiting cases of $Da \rightarrow 0$ (slug flow) and $Da \rightarrow \infty$ (Free flow).

The above graph shows the change in Nusselt number with the dimensionless axial coordinate along the length of the duct. Considering the flow direction it is observed that there is a decrease in Nusselt number as we go across farther from zero showing the effect of axial conduction reducing on the flow. The Nusselt number is the ratio of the effect of convection to that of conduction. Thus, it gives an idea of how much conduction or convection is entering into the system and by looking at the graph the effect of conduction lowers as we go away from x=0.

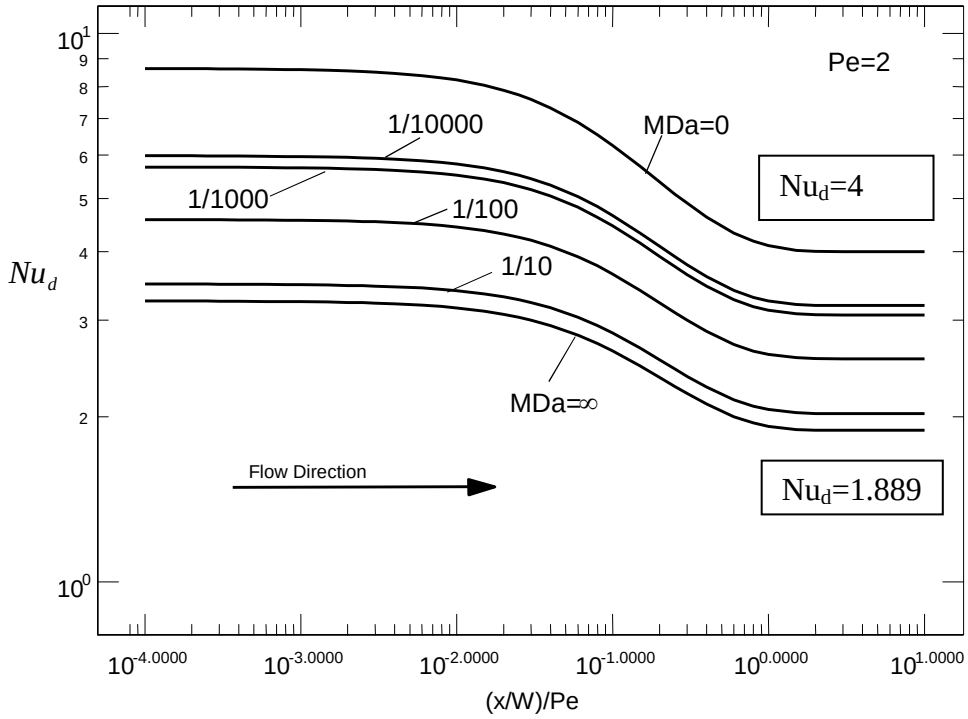

Figure 3.2 Computed Nu_d as a function of dimensional axial coordinate for Pe=2. The values displayed on the right hand side of the figure are the fully developed values (attained asymptotically as $x \rightarrow \infty$) for the limiting cases of $Da \rightarrow 0$ (slug flow) and $Da \rightarrow \infty$ (Free flow).

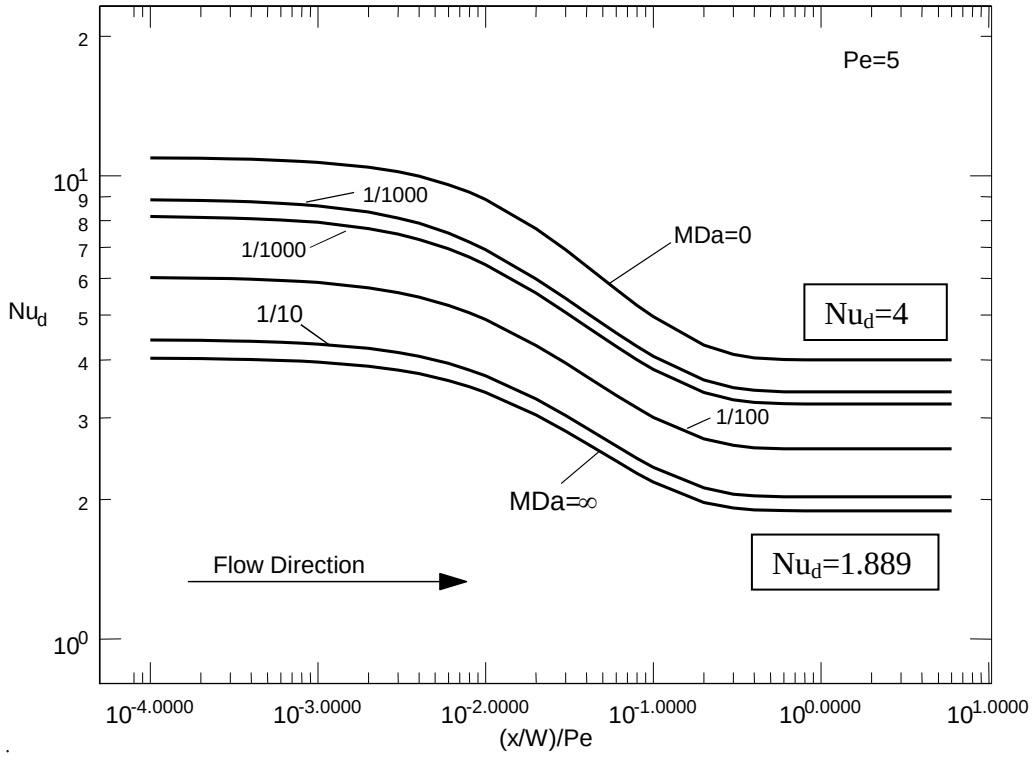

Figure 3.3 Computed Nu_d as a function of dimensionless axial coordinate for Pe=5. The values displayed on the right hand side of the figure are the fully developed values (attained asymptotically as $x \rightarrow \infty$) for the limiting cases of $Da \rightarrow 0$ (slug flow) and $Da \rightarrow \infty$ (Free flow).

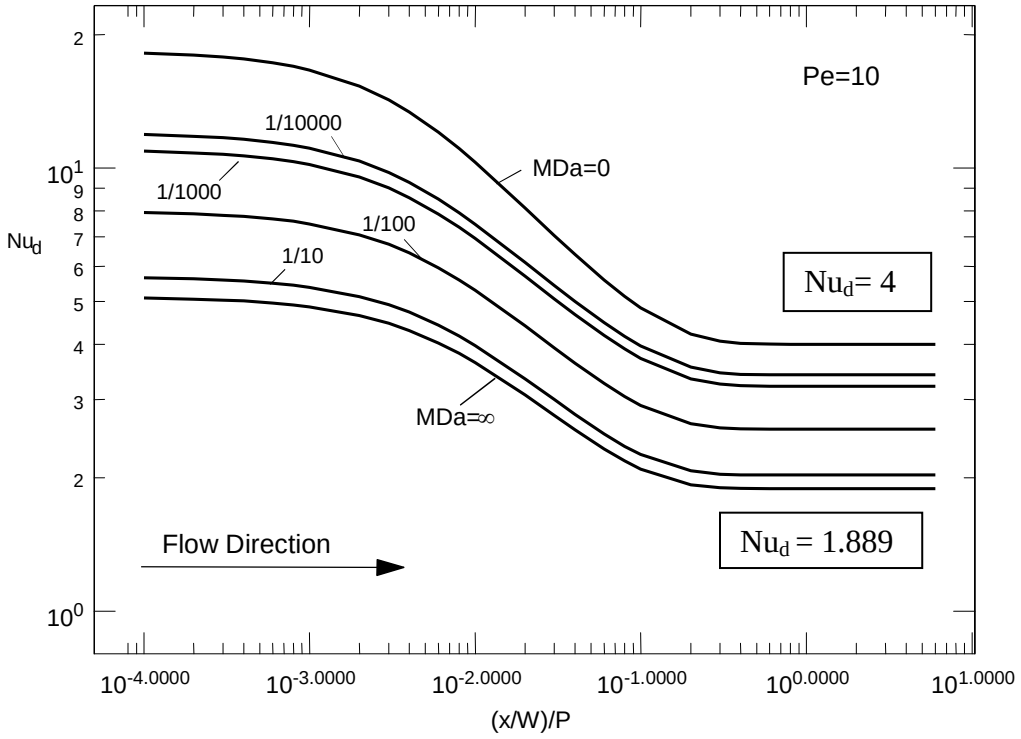

Figure 3.4 Computed Nu_d as a function of dimensionless axial coordinate for Pe=10. The values displayed on the right hand side of the figure are the fully developed values (attained asymptotically as $x \rightarrow \infty$) for the limiting cases of $Da \rightarrow 0$ (slug flow) and $Da \rightarrow \infty$ (Free flow).

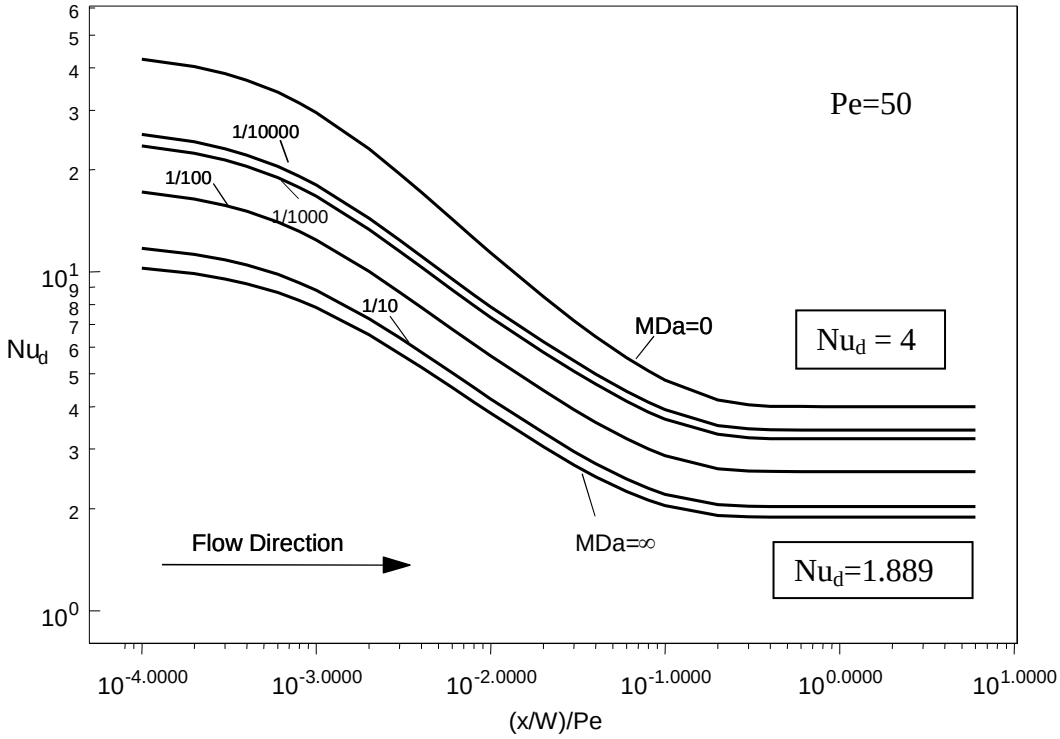

Figure 3.5 Computed Nu_d as a function of dimensionless axial coordinate for Pe=50. The values displayed on the right hand side of the figure are the fully developed values (attained asymptotically as $x \rightarrow \infty$) for the limiting cases of $Da \rightarrow 0$ (slug flow) and $Da \rightarrow \infty$ (Free flow).

The above graphs show the variations in Nusselt number with the axial coordinate when the Peclet Number (Pe) increases. At Pe=50, the effect of axial conduction becomes very less. It can also be seen that the wall temperature and bulk temperature of the fluid varies with the different values of Peclet number and MDa. The effect of axial conduction can be seen from the graph when x<0 and the penetration can be observed. The graphs are displayed in the following section.

3.2 Wall temperature vs. axial coordinate

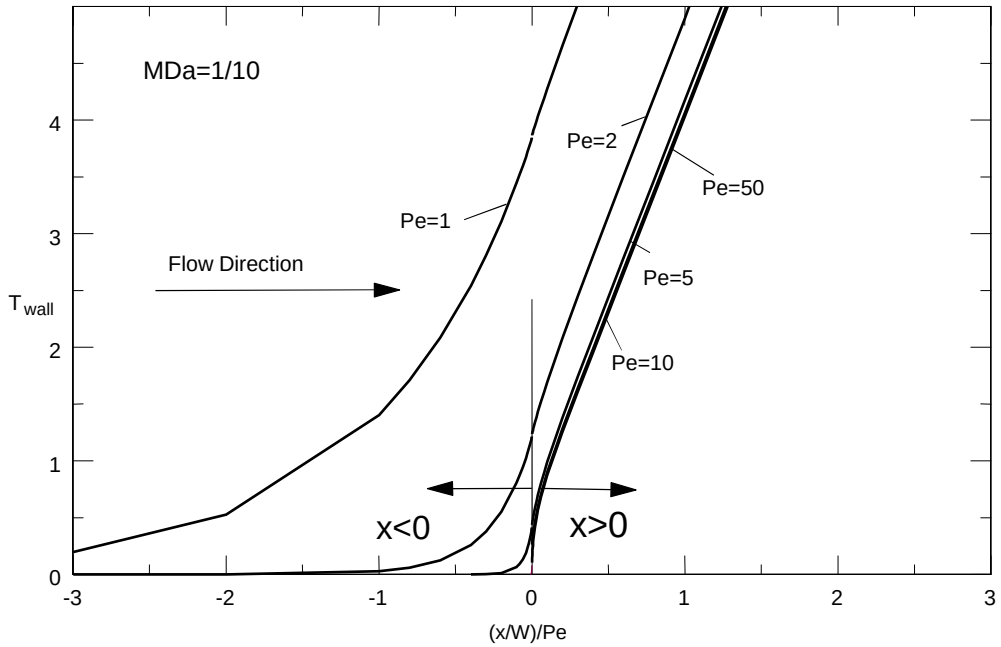

Figure 3.6 Wall temperature as a function of dimensionless axial coordinate for MDa=1/10

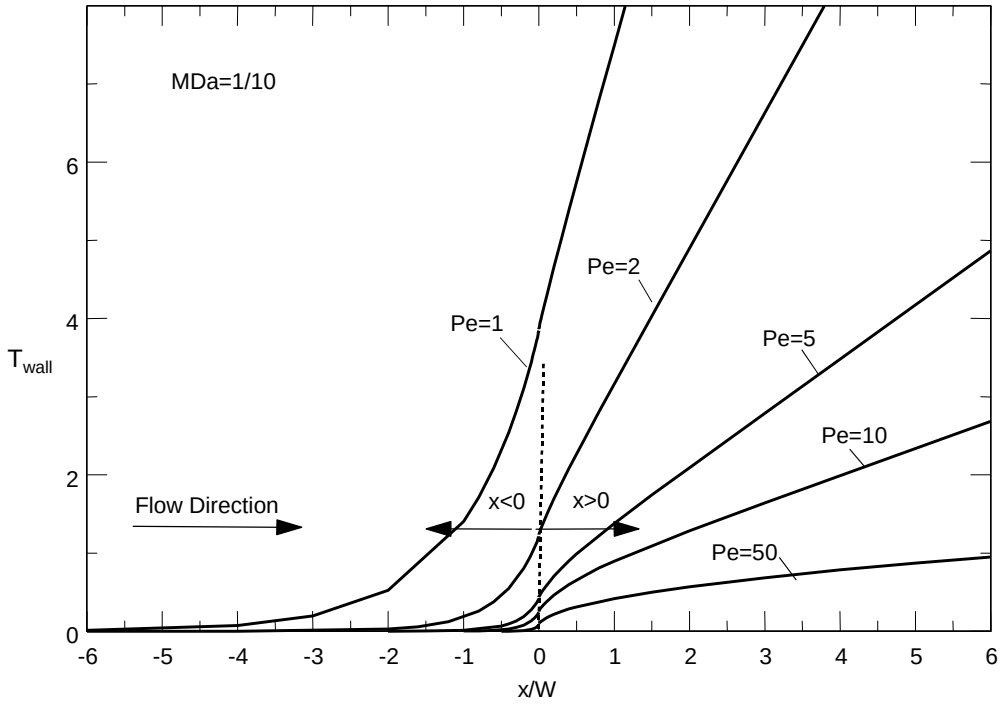

Figure 3.7 Wall temperature as a function of axial coordinate x/W for MDa=1/10

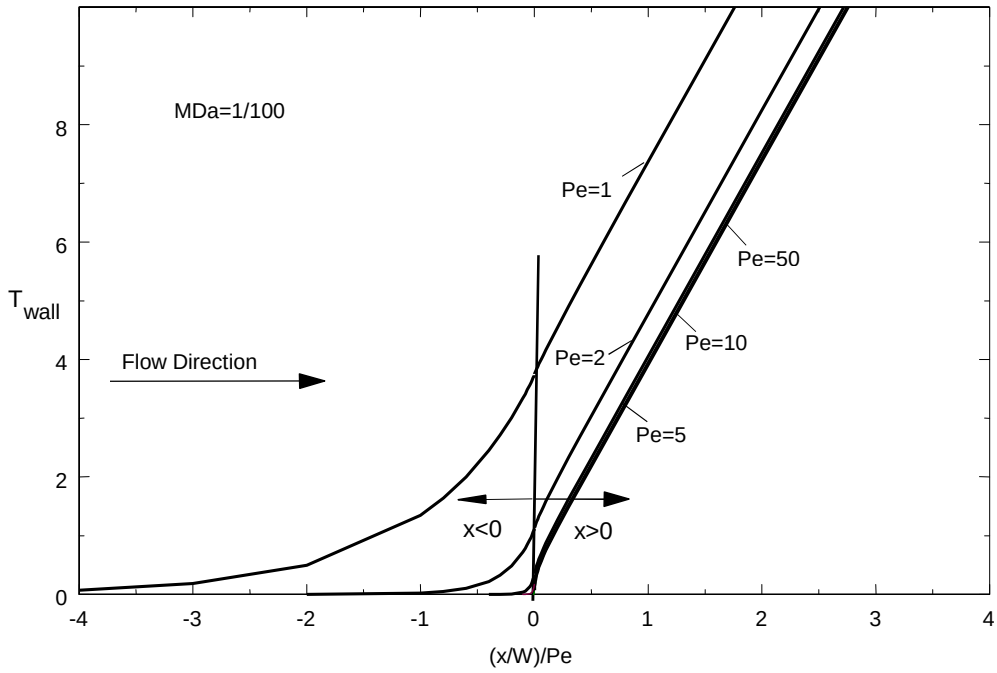

Figure 3.8 Wall temperature as a function of axial coordinate (x/W)/Pe for MDa=1/100

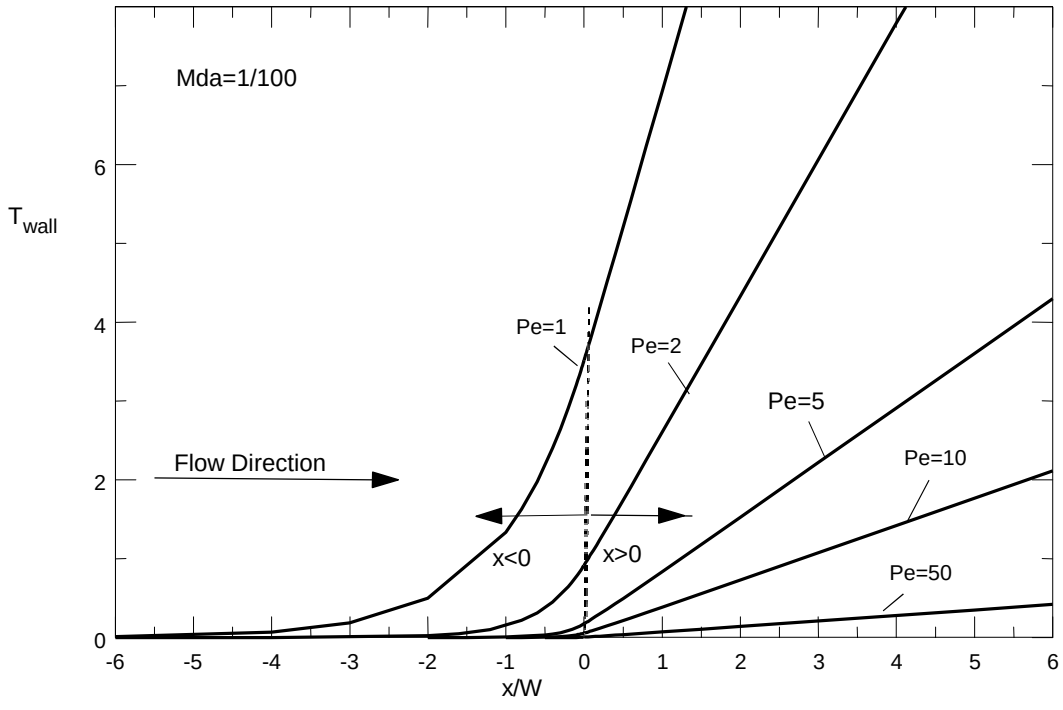

Figure 3.9 Wall temperature as a function of axial coordinate x/W for MDa=1/100

3.3 Bulk Temperature vs. axial coordinate

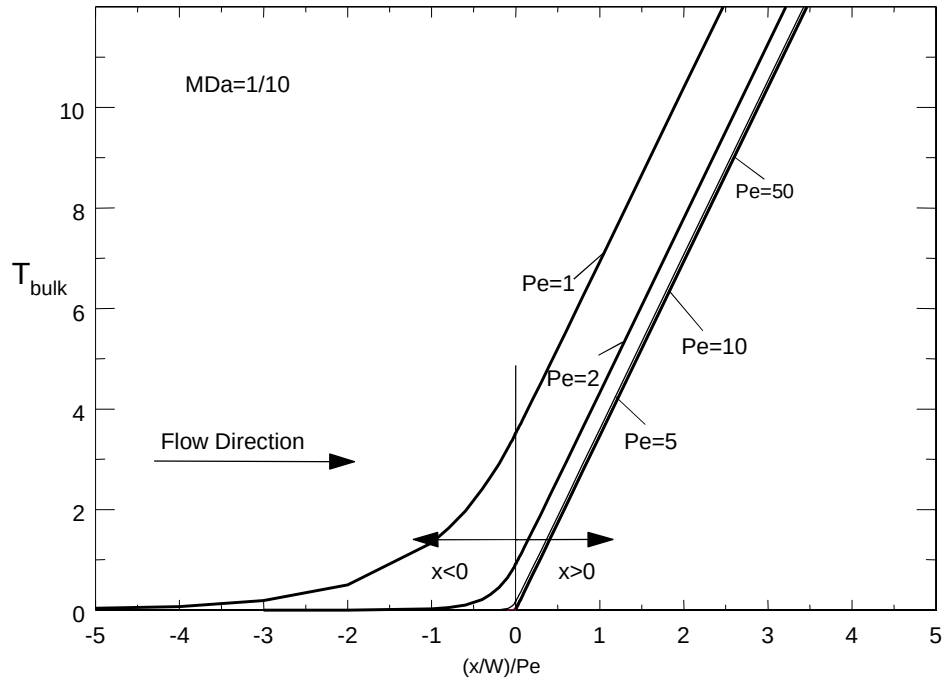

Figure 3.10 Bulk temperature as a function of dimensionless axial coordinate for MDa=1/10

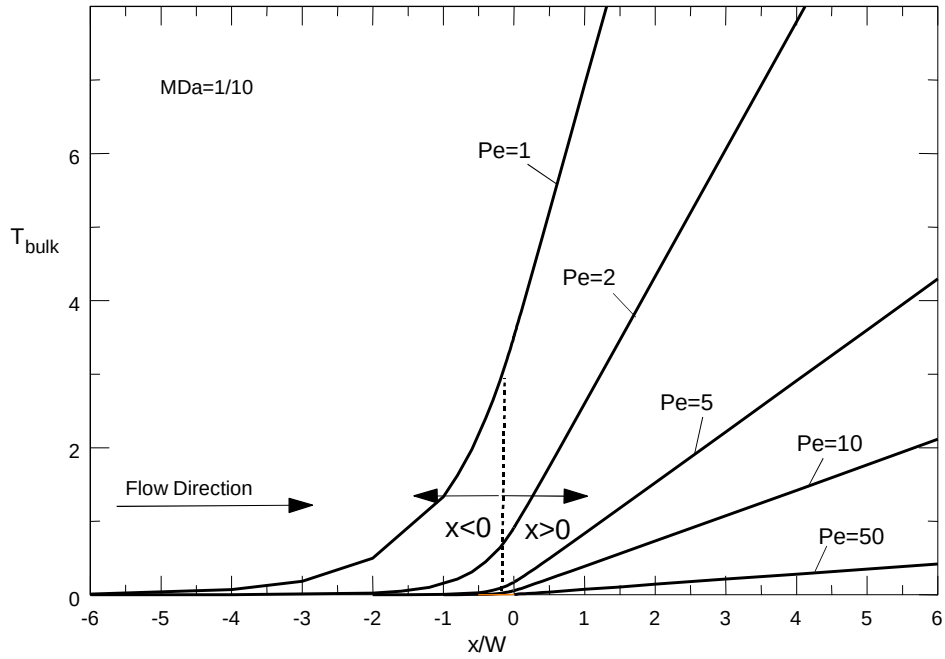

Figure 3.11 Bulk temperature as a function of axial coordinate x/W for MDa=1/10

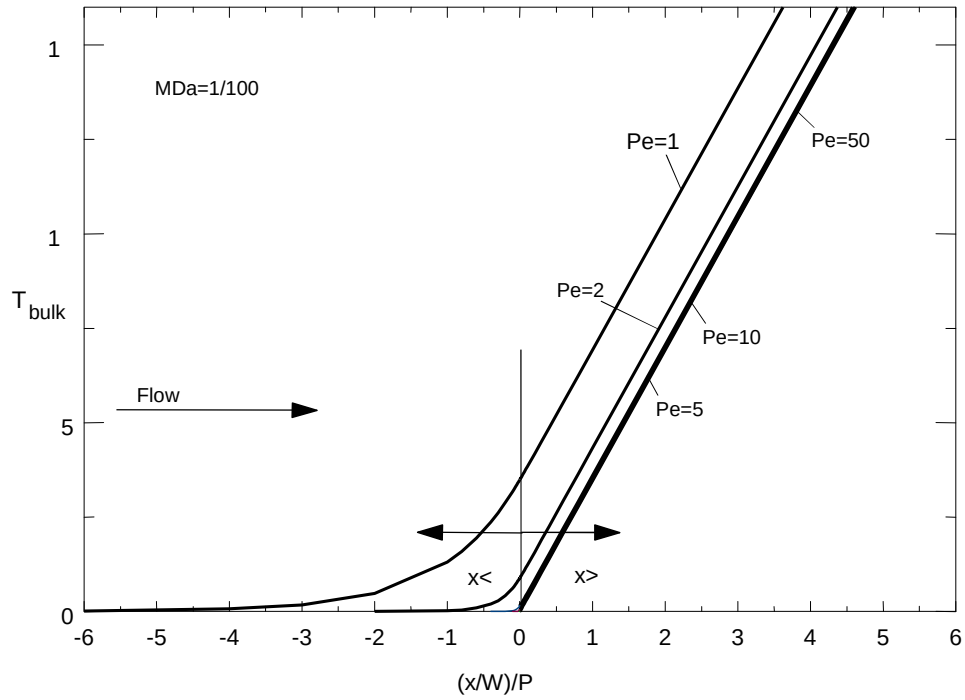

Figure 3.12 Bulk temperature as a function of dimensionless axial coordinate for MDa=1/100

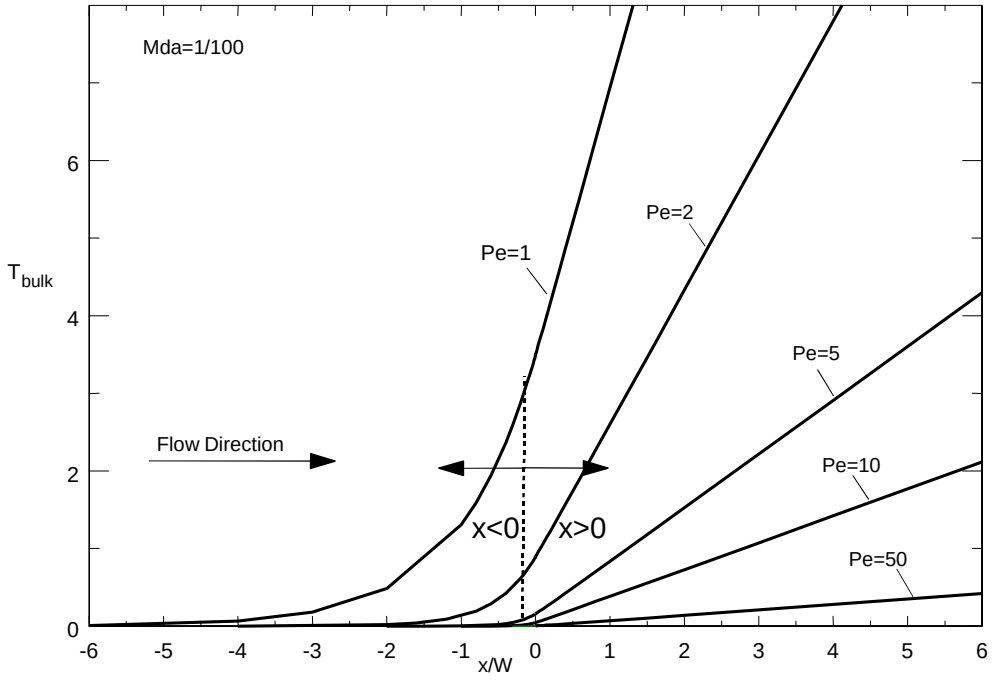

Figure 3.13 Bulk temperature as a function of axial coordinate x/W for MDa=1/100

3.4 Temperature Profile

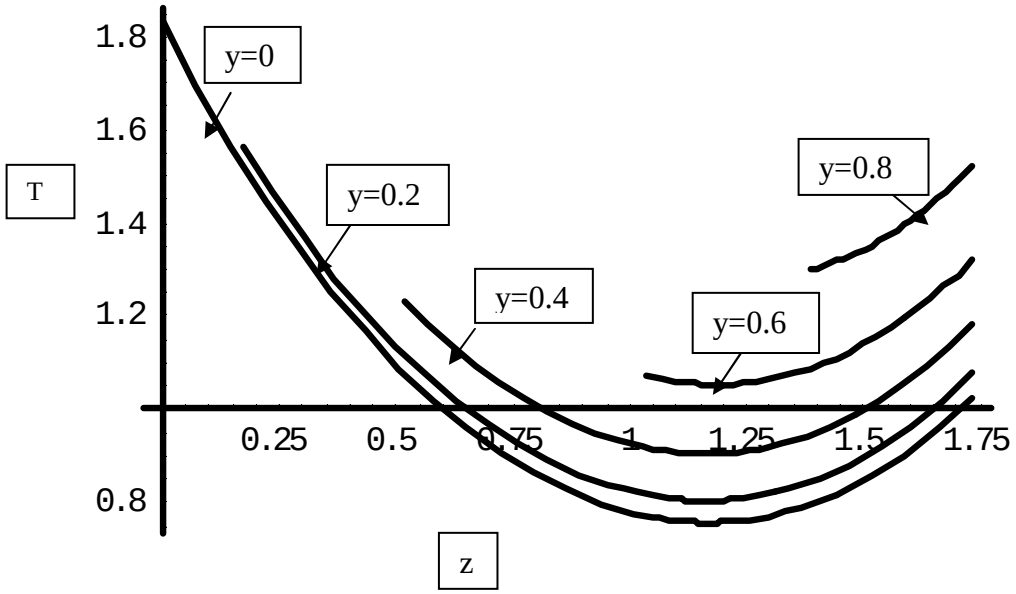

Figure 3.14 Temperature profile of flow plotted against the z-coordinate as x->0 and y is a taken as a parameter having different values between 0 and 1.

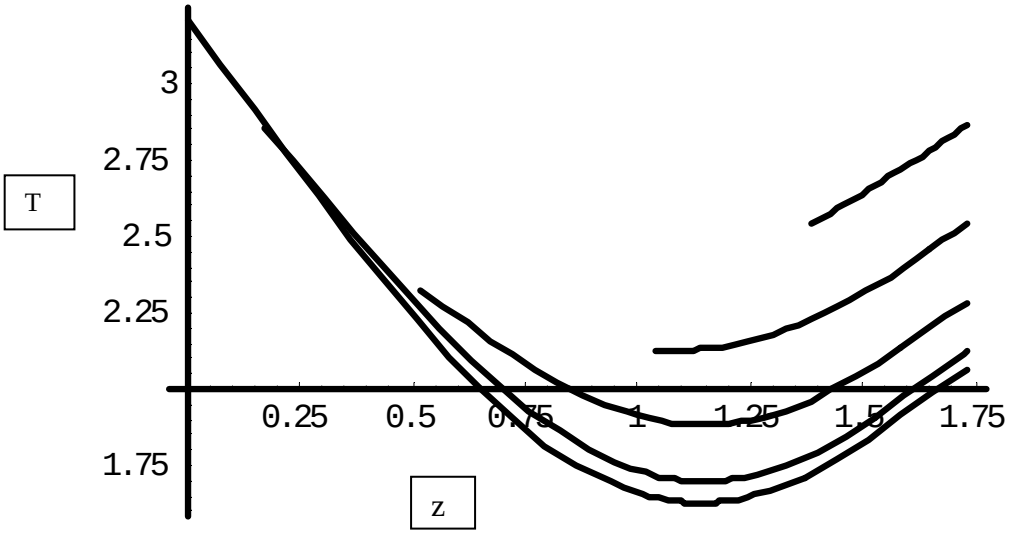

Figure 3.15 Temperature profile of flow plotted against the z-coordinate as x->0.3 and y is a parameter having different values between 0 and 1.

The above section displays the temperature field against the vertical coordinate z. As can be seen from the graph the temperature field increases in the z direction as the average wall and bulk temperature increase. As we progress in the vertical direction the temperature profile increases aided by the constant wall heat flux condition which increases the temperature profile. The slope of the graph has a dip initially and the temperature lowers as we go upwards from the base but increases as we reach the top portion. As we increase the x-coordinate of the flow the graph is seen to be shifted to the right and gets elevated

The above graphs show the influence of axial conduction on wall temperature and bulk temperature at $x<0$ for boundary conditions of the second kind. As seen from the Fig.3.6-3.9 referring to wall temperature the effect of Darcy number (Da) is small at $x=0$ and its effect increases as x increases. As seen from the figures the temperature at $x<0$ increases significantly for Pe=10 as compared to Pe=50.Thus, there is a substantial increase in temperature penetration upstream as Pe reduces. The effect of axial conduction is seen to be maximum at $x=0$ and reduces as we go downstream. The thermal entrance length reduces as the MDa values decrease and the slope of bulk temperature increases.

Looking at the Figs.3.10-3.13 gives us an idea of the behavior of the bulk temperature graphs around the $x=0$ region. We can observe that the bulk temperature values near $x=0$ increase as the Peclet number decreases. Thus we require more number of eigenvalues and basis functions at $x=0$ for increased accuracy. The various eigenvalues used with different MDa values such as 1/10, 1/100, 1/1000 etc. in the computations are listed below .Similar negative eigenvalues are present which are used for plotting the parameters such as wall and bulk temperature at $x<0$.The eigenvalues are plotted in a tabular form and displayed in the next section

3.5 Tables containing positive and negative Eigenvalues computed by Mathematica

Table 3.1 Positive Eigenvalues for MDa=1/10 and order =9 in the temperature field solution

N	Pe=1	Pe=2	Pe=5	Pe=10	Pe=50	Pe=100
1	26.161	51.644	124.426	235.225	830.807	1208.82
2	24.656	48.597	116.499	218.348	746.7	1071.09
3	23.723	46.470	109.704	202.023	664.559	939.782
4	22.957	44.741	104.145	188.706	589.517	818.923
5	21.526	42.145	98.602	176.936	521.826	785.725
6	19.176	37.683	89.619	165.213	499.311	717.307
7	17.688	34.599	82.498	153.441	482.627	677.275
8	17.535	34.372	79.739	142.387	473.475	581.456
9	16.364	31.809	73.445	132.541	369.208	434.837
10	15.063	29.380	69.417	127.303	327.713	402.031
11	14.688	28.814	67.417	120.134	306.202	359.323
12	13.523	27.458	64.349	115.045	289.976	336.072
13	12.9552	26.109	59.9715	106.819	265.8	293.252
14	11.5517	25.0868	57.1816	99.6606	254.751	290.839
15	10.672	23.472	54.4969	98.9206	217.81	237.832
16	10.2493	22.5906	51.7751	87.6704	176.129	191.631
17	9.37022	20.6582	46.8779	79.7923	150.905	165.159
18	8.7848	19.6386	43.6567	73.5173	148.637	160.126
19	7.9638	17.8524	39.1775	66.3155	142.58	151.868

Table 3.2 Positive Eigenvalues for MDa=1/100 and order =9 in the temperature field solution

N	Pe=1	Pe=2	Pe=5	Pe=10	Pe=50	Pe=100
1	26.1411	51.5513	123.726	232.099	769.598	1049.882
2	24.6534	48.5018	115.83	215.524	683.887	906.888
3	23.7559	46.574	109.908	201.187	599.86	771.296
4	23.089	45.0066	105.188	189.546	526.298	658.081
5	21.4975	42.0516	98.2844	176.585	464.029	597.399
6	19.1431	37.5393	88.6579	161.956	438.712	537.602
7	17.699	34.531	80.8899	147.429	416.008	515.123
8	17.473	34.2302	79.9691	142.441	403.523	513.579
9	16.3876	31.8837	73.6002	130.441	345.742	391.982
10	15.0505	29.2929	68.3291	124.576	306.264	343.842
11	14.6324	28.5974	66.4927	117.195	276.04	312.673
12	14.3305	27.8907	64.3744	113.588	250.177	284.927
13	13.4488	26.0769	59.5945	103.876	247.716	269.92
14	12.9719	25.1362	57.3608	99.2918	230.228	253.632
15	12.1098	23.4434	53.6951	95.9538	205.55	221.429
16	11.5044	22.4223	51.4878	87.5172	166.795	177.061
17	10.6498	20.5531	46.235	77.7563	140.876	147.531
18	10.2619	19.6686	43.4897	71.9301	129.728	136.501
19	9.3918	17.9327	39.2314	64.951	116.182	122.166

Table 3.3 Positive Eigenvalues for MDa=1/1000 and order =9 in the temperature field solution

N	Pe=1	Pe=2	Pe=5	Pe=10	Pe=50	Pe=100
1	26.1114	51.4282	122.902	228.651	703.775	899.095
2	24.601	48.36	114.907	211.794	616.625	761.958
3	23.7622	46.5847	109.805	199.839	545.361	654.288
4	23.0709	45.1646	105.957	191.149	490.373	571.078
5	21.5055	42.0865	98.6436	177.623	445.423	514.058
6	19.1078	37.3874	87.5982	157.666	388.847	440.119
7	17.6955	34.0586	80.0992	142.628	363.912	436.699
8	17.4197	34.0273	79.3644	141.664	332.004	377.711
9	16.3964	31.9115	73.6189	129.443	319.704	366.329
10	15.0503	29.2633	67.534	120.329	291.099	322.179
11	14.579	28.3849	65.6317	115.453	256.318	281.662
12	14.3188	27.8449	63.9489	111.183	230.264	247.492
13	13.4351	26.0206	59.1614	101.652	215.07	237.289
14	12.9716	25.1239	57.1875	98.4799	203.175	218.826
15	12.1122	23.4478	53.3026	92.4871	196.415	209.54
16	11.4503	22.2228	50.802	87.1111	163.459	172.165
17	10.6157	20.4094	45.3697	75.0588	130.958	136.545
18	10.2675	19.6798	43.3725	70.9138	120.356	125.084
19	9.4113	18.0048	39.4812	64.1338	107.162	111.137

Table 3.4 Negative Eigenvalues for MDa=1/100 and order =9 in the temperature field solution

N	Pe=1	Pe=2	Pe=5	Pe=10	Pe=50	Pe=100
1	-26.9102	-54.6324	-143.186	-313.527	-3777.46	-14375.1
2	-25.4473	-51.7644	-137.134	-308.896	-3625.59	-14177.2
3	-24.754	-50.5556	-134.21	-297.489	-3591.81	-14024.343
4	-24.1312	-49.414	-132.495	-292.11	-3551.06	-13743.81
5	-22.4742	-45.9589	-122.83	-274.673	-3502.11	-13609.52
6	-19.9456	-40.7625	-109.338	-250.183	-3404.43	-13260.8
7	-18.6209	-38.2086	-103.249	-238.435	-3340.23	-12827.3
8	-18.2199	-37.2298	-99.5318	-225.274	-3313.28	-12816.4
9	-17.3369	-35.6775	-97.1066	-220.247	-3276.42	-12673.7
10	-15.9649	-32.9458	-91.0138	-217.438	-3173.19	-12341.7
11	-15.3805	-31.6564	-87.2738	-209.161	-3012.98	-11450.9
12	-15.114	-31.0002	-84.0451	-200.521	-2906.4	-10986.2
13	-14.3188	-29.5431	-80.6319	-196.63	-2849.15	-10665.7
14	-13.8596	-28.705	-80.1948	-180.45	-2776.4	-10336.5
15	-12.9234	-26.7076	-73.0781	-179.963	-2689.68	-9966.25
16	-12.1176	-24.9139	-69.5594	-177.13	-2567.2	-8829.74
17	-11.4705	-23.8857	-68.4692	-166.375	-2127.16	-7434.2
18	-11.1917	-23.3607	-65.2379	-163.948	-1860.67	-6758.62
19	-10.31	-21.5783	-60.8809	-152.788	-1784.57	-6349.24

Table 3.5 Negative Eigenvalues for MDa=1/1000 and order =9 in the temperature field solution

N	Pe=1	Pe=2	Pe=5	Pe=10	Pe=50	Pe=100
1	-26.9372	-54.733	-143.626	-312.553	-3265.61	-12296.1
2	-25.4772	-51.8663	-136.892	-301.318	-3216.82	-12138.9
3	-24.7429	-50.5081	-134.351	-297.643	-3155.68	-11978.2
4	-24.0857	-49.2238	-131.323	-292.593	-3146.57	-11916.8
5	-22.4678	-45.9369	-122.759	-274.786	-3089.75	-11785.2
6	-19.9732	-40.8517	-109.364	-246.441	-3072.85	-11728.2
7	-18.6242	-38.225	-103.382	-236.274	-3049.04	-11624.6
8	-18.2751	-37.4521	-100.907	-230.024	-3021.55	-11446.2
9	-17.3251	-35.6274	-96.8893	-222.892	-3005.5	-11353.2
10	-15.9528	-32.8746	-90.1457	-211.738	-2983.49	-11331.9
11	-15.4157	-31.7365	-86.8215	-203.636	-2920.19	-11236.6
12	-15.1372	-31.1244	-84.6744	-197.65	-2885.73	-11140.3
13	-14.3345	-29.6183	-81.6359	-191.518	-2852.69	-11077.1
14	-13.851	-28.6465	-79.4092	-188.997	-2816.89	-10871.2
15	-12.9339	-26.7322	-73.7213	-173.09	-2763.84	-10691.1
16	-12.1744	-25.1292	-69.4442	-169.16	-2725.5	-10102.3
17	-11.492	-23.9172	-67.4353	-165.99	-2513.2	-9204.36
18	-11.1834	-23.3428	-66.2046	-159.903	-2350.48	-8936.65
19	-10.2924	-21.5295	-61.5152	-151.903	-2265.67	-8362.1

CHAPTER 4

CONCLUSION AND FUTURE WORK

4.1 Conclusion

An analytical approach is applied for the determination of velocity field and temperature field in triangular ducts. Boundary conditions of second kind (H2) are taken into consideration in addition to the inclusion of axial conduction. A weighted residual method namely the Galerkin method was used for the computations pertaining to the velocity field. For hydrodynamic fully developed flow, the velocity in triangular passages is a function of y and z. However, in the thermal entrance region, the computation of the temperature field becomes more demanding since the temperature depends on x, y, z.

An extended weighted residual method was used for determination of temperature field. The calculation of eigenvalues and eigenvectors for determining the temperature distribution has been done by using a Mathematica program as presented in Appendix A. The tabulated eigenvalues in the previous chapter refer to the positive and negative eigenvalues which have been used to determine the temperature field and produces the graphs seen in Chapter 3 and in other computations.

To show the effect of axial conduction a number of graphs were presented and the behavior of parameters such as Nusselt number, average wall temperature and bulk temperature were examined closely at the region in and around x=0. The Nusselt number is a non-dimensional measure of the rate of heat transfer into the bulk of the fluid. It is observed that the Nusselt number is very closely related with the Peclet number of the flow. When the value of Peclet number is small at x=0, the effect of axial conduction is prominent and the value of Nusselt

number decreases near the x=0 location. We can also observe that the plot for Pe =10 is very close to that with Pe=50 demonstrating that the effect of axial conduction is small after x=10.

The Nusselt number for large values of the axial coordinate approaches the fully developed value which in this case is 1.889 for clear flow. This indicates a different behavior in comparison to the case for a step change in wall temp in [15] where Nu_d increases as Pe decreases.

Keeping this in mind neglecting the contribution of axial conduction in the case of prescribed wall heat flux can overestimate the values near the thermal entrance region.

Also by observing the graphs displayed in section 3.2 and 3.3, one can notice the wall and bulk temperature changes in and around x=0. The dimensionless parameter MDa represents a relative measure of the permeability of the porous media. For intermediate values of MDa, velocity profiles are characterized by a higher wall velocity gradient and a flat profile near the center of the channel.

The effect of Darcy number on bulk temperature is relatively small when ((x/W)/Pe) is small and it decreases as the axial coordinate increases for a range of Peclet numbers. The wall temperature is influenced by the MDa as well as the Peclet number which can be observed from Fig.3.10-3.13.There is maximum penetration at lower values of Pe as the axial conduction is higher and the upstream penetration increases. The linear nature of the graphs referring to wall and bulk temperature at x>0 increases as the Pe increases for larger values of the axial coordinate .As for the x<0 region it takes some time for the profile to become linear for lower values of Peclet numbers. The effect of axial conduction reduces and the thermal penetration is very small for Pe =10 and Pe= 50.

4.2 Future Work

We have seen the computations of temperature and velocity fields for triangular ducts with boundary conditions of the second kind being determined by the use of Galerkin method. There

is however a change in the computations when an isosceles duct is not taken into consideration, that is if the included angle is something other than 30°. Also if the edges are rounded the calculation changes as the dimensions of the triangle are changed. Thus, there remain modifications to the solution which can be achieved with the inclusion of these factors. Viscous Dissipation is also been neglected in this analysis. The inclusion of viscous dissipation can also be one of the additions and would not be that tedious since axial conduction has already been considered.

APPENDIX A

MATHEMATICA INPUT FOR SOLVING VELOCITY AND TEMPERATURE FIELD FOR AN ISOSCELES TRIANGLE

```
SetPrecision[All,1000];
Off[General::spell1];Off[Solve::svars];
(*INPUT DATA*)

Clear[y, z, q, i]
da=1/10;
m=1;
h=Sqrt[3];
w=1;
m0=3;
n0=5;
cap=1;
mn0=m0*n0;
area=w*h/2;
perim= w+Sqrt[h^2+w^2];
dhyd= 4*area/perim;

(*BASIS FUNCTIONS*)

fi=(z^2-(h*y/w)^2)*(z-h)*z^(q-1)*y^(2 i-2);

(*CALCULATIONS*)

Do[Do[i1=(i-1)*n0+q;fvi[i1]=fi,{q,1,n0}],{i,1,m0}];
Do[Do[i1=(i-1)*n0+q;fvj[i1]=fi,{q,1,n0}],{i,1,m0}];
md=1/(da*m);
psi0=-1/m;
Do[Do[
    operfj[i1,j1]=fvi[i1]*(D[D[fvj[j1],y],y]+D[D[fvj[j1],z],z]-md*fvj[j1]),{j1,1,mn0}],{i1,1,mn0}];
psivect=Table[Integrate[Integrate[fvi[i1]*psi0,{z,h*y/w,h}],{y,0,w}],{i1,1,mn0}];
amat=Table[Integrate[Integrate[operfj[i1,j1],{z,h*y/w,h}],{y,0,w}],{j1,1,mn0},{i1,1,mn0}];
cvect=Inverse[amat].psivect;
fvect=Table[fvj[j],{j,1,mn0}];
u=cvect.fvect;

(*CALCULATIONS OF THE VELOCITY FIELD*)

uav=2*Integrate[Integrate[u,{z,h*y/w,h}],{y,0,w}]/(h*w);m0=3;
Clear[q,i];
(*Calculations*)
order=9;
```

```
tab=Table[Table[z^i y^(n-i),{i,0,n}],{n,0,order}];
base=Flatten[tab];
poly=base.Table[c[i],{i,Length[base]}];
len=Length[poly];
solpoly=DeleteCases[Table[Coefficient[Expand[poly/.sol], c[i]],{i,1,len}],0]


(*SOLVING MATRICES A, B, C FOR CALCULATION OF EIGENVALUES*)

mn0=29;
Do[fvi[j]=solpoly[[j]],{j,1,mn0}]
Do[fvj[j]=solpoly[[j]],{j,1,mn0}]
Do[Do[
    operfj[i1,j1]=Expand[fvi[i1]*(D[D[fvj[j1],y],y]+D[D[fvj[j1],z],z])],{j1,1,mn0}],{i1,1,mn0}];
amat=Table[Integrate[Integrate[operfj[i1,j1],{z,h*y/w,h}],{y,0,w}],{j1,1,mn0},{i1,1,mn0}];
redm=Table[Integrate[Integrate[operfj[i1,j1],{z,h*y/w,h}],{y,0,w}],{j1,2,mn0},{i1,2,mn0}];
u1=Simplify[u/uav];
Do[Do[
    fifj[i1,j1]=Simplify[Expand[u1*fvi[i1]*fvj[j1]]],{j1,1,mn0}],{i1,1,mn0}];
bmat=Table[Integrate[Integrate[cap*fifj[i1,j1],{z,h*y/w,h}],{y,0,w}],{j1,1,mn0},{i1,1,mn0}];
Do[Do[
    fifj[i1,j1]=Simplify[Expand[fvi[i1]*fvj[j1]]],{j1,1,mn0}],{i1,1,mn0}];
cmat1=Table[Integrate[Integrate[fifj[i1,j1],{z,h*y/w,h}],{y,0,w}],{j1,1,mn0},{i1,1,mn0}];
pe=5;
cmat=cmat1/pe^2;
{eigv,dvmt}=Eigensystem[abar];
pcoef=Inverse[Transpose[dvmt.bm]];
N[eigv];
jj=0;

Do[If[eigv[[i1]]□0,jj=jj+1];If[eigv[[i1]]□0,pg[jj]=eigv[[i1]]];If[eigv[[i1]]□0,Do[dd[jj,j1]=dvmt[[i1,j1]],{j1,
1,n}]],{i1,1,2*n}];
pose=Table[pg[i],{i,1,jj}];
posdmt=Table[dd[j1,i1],{j1,1,n},{i1,1,n}];
jjn=0;
Do[If[eigv[[i1]]□0,jjn=jjn+1];
```

```
   If[eigv[[i1]]□0,ng[jjn]=eigv[[i1]]];If[eigv[[i1]]□0,Do[dd[jjn,j1]=dvmt[[i1,j1]],{j1,1,n}]],{i1,1,2*n}];
nege=Table[ng[i],{i,1,jjn}];
negdmt=Table[dd[j1,i1],{j1,1,n},{i1,1,n}];
 (*Remove[pg,ng,dd,amat,aaa,bbb,abar,am,bm];*)
N[pose]
N[nege]

(*DETERMINATION OF NUSSELT NUMBER, BULK AND WALL TEMPERATURE*)

Clear[x];
u1=u/uav;
qwovk=1;
dvmt=posdmt;
eigv=pose;
compT=(w+Sqrt[w^2+h^2])*(y^2+z^2)/2/h-Sqrt[w^2+h^2]*z;
sr=2*(w+Sqrt[h^2+w^2])/h;
psivect=Table[Integrate[Integrate[Expand[fvi[i1]*(4*u1/dhyd-sr)],{z,h*y/w,h}],{y,0,w}],{i1,2,mn0}];
aaa=N[redm,800];
cvect=Inverse[aaa].psivect;
fvect=Table[fvj[j],{j,2,mn0}];
phi=cvect.fvect;
ufact=phi+compT;
cf1=Integrate[Integrate[ufact*u1,{z,h*y/w,h}],{y,0,w}]/area;
ufact=ufact-cf1;
psivt1=Table[Integrate[Integrate[Expand[fvi[i1]*ufact*u1],{z,h*y/w,h}],{y,0,w}],{i1,1,mn0}];
psivt2=Table[Integrate[Integrate[(4/dhyd)*fvi[i1],{z,h*y/w,h}],{y,0,w}],{i1,1,mn0}];
psivt3=Table[Integrate[Integrate[fvi[i1]*ufact,{z,h*y/w,h}],{y,0,w}],{i1,1,mn0}];
temp=0;
temp=temp+(4 x/dhyd)+ufact;
tbulk=(1/area)*Integrate[Integrate[Expand[temp*u1],{z,h*y/w,h}],{y,0,w}];
tbulk=Simplify[Expand[tbulk]];
twall=(Integrate[Sqrt[1+h^2/w^2]*temp/.z□h*y/w,{y,0,w}]+Integrate[temp/.z□h,{y,0,w}])/perim;
nu=dhyd*qwovk/(twall-tbulk);
```

REFERENCES

[1] Sparrow, E. M., and Siegel, R., 1959, “A Variational Method for Fully Developed Laminar Heat Transfer in Ducts,” ASME J. Heat Transfer, Vol. 81, No.2, pp. 157–167.

[2] Haji-Sheikh, A., Mashena, M., and Haji-Sheikh, M.J.,”Heat Transfer Coefficient in Ducts with Constant Wall Temperature”, ASME Journal of Heat Transfer, Vol. 105, No.4, 1983, pp. 878-883.

[3] B. Weigand , M. Kanzamar and H. Beer ., The extended Graetz problem with piecewise constant wall heat flux for pipe and channel flows, International Journal of Heat and Mass Transfer, Volume 44, No. 20, 2001, pp. 3941-3952

[4] R.K. Shah ,Laminar Flow Friction and Forced Convection Heat Transfer in Ducts of Arbitrary Geometry, Int. J. Heat Mass Transfer, vol. 18,No.7-8,1974, pp. 849–862,

[5] Lakshminarayanan, R. and Haji-Sheikh, A., “Entrance Heat Transfer in Isosceles and Right Triangle Ducts”, AIAA J. of Thermophysics and Heat Transfer, Vol. 6, No.1, 1992, pp.167-171.

[6] D.A. Nield, A.V. Kuznetsov, Forced convection in porous media: transverse heterogeneity effects and thermal development, in: K.Vafai (Ed.), Handbook of Porous Media, second ed., Taylor and Francis, New York, 2005, pp. 143–193.

[7] A. Haji-Sheikh, K. Vafai, Analysis of flow and heat transfer in porous media imbedded inside various-shaped ducts, Int. J. Heat Mass Transfer, Vol.47, No.8-9, 2004, pp. 1889–1905.

[8] K. Hooman, Fully developed temperature distribution in porous saturated duct of elliptical cross-section, with viscous dissipation effects and entropy generation analysis, Heat Transfer Res,Vol. 36 ,2005 , pp. 237–245.

[9] K. Hooman, H. Gurgenci, Effects of temperature-dependent viscosity variation on entropy generation, heat, and fluid flow through a porous-saturated duct of rectangular cross-section, Applied Math Mech., Volume 28,No. 1, pp.69-78.

[10] Hooman, K., and Merrikh, A. A., 2006, “Analytical Solution of Forced Convection in a Duct of Rectangular Cross Section Saturated by a Porous Medium,” ASME J. Heat Transfer, Volume 128, No.6, pp. 596–600.

[11] Haji-Sheikh, A., Minkowycz, W. J., and Sparrow, E. M., 2004, “A Numerical Study of the Heat Transfer to Fluid Flow Through Circular Porous Passages,” Numerical Heat Transfer, Part A, Volume 46, No.10, pp. 929–956.

[12] A. Haji-Sheikh a,*, E.M. Sparrow b, W.J. Minkowycz c, Heat Transfer to flow through Porous Passages using Extended Weighted Residual Method-a Green’s Function Solution., Intl. J. of Heat and Mass Transfer ,Vol.48, No. 7, 2005, pp.1330–1349.

[13] Hooman, K and Haji-Sheikh, A., “Analysis of heat transfer and entropy generation for a thermally developing Brinkman–Brinkman forced convection problem in a rectangular duct with isoflux walls”, International Journal of Heat and Mass Transfer, Vol. 50, No.21-22, 2007, pp.4180–4194.

[14] Lahjomri, J., and Oubarra, A., 1999, “Analytical Solution of the Graetz Problem with Axial Conduction,” ASME J. Heat Transfer, Vol.121, No.4, pp. 1078–1083.

[15] Minkowycz, W. J., and Haji-Sheikh, A., 2006, “Heat Transfer in Parallel-Plate and Circular Porous Passages with Axial Conduction,” Int. J. Heat Mass Transfer, Vol. 49, No.13–14, pp. 2381–2390.

[16] Haji-Sheikh, A., Determination of heat transfer in ducts with axial conduction by variational calculus, ASME J. Heat Transfer, Vol. 131, No. 9 , 2009, 09-1702-(1-11).

[17] Lundgren, T. S. , Slow Flow Through Stationery Random Beds and Suspensions of Spheres, J. of Fluid Mechanics, Vol. 51, No.2 , 1972 , pp. 273-299.

[18] Meirovitch, L.,Analytical Methods in Vibrations, McMillan Company, New York,1967

BIOGRAPHICAL INFORMATION

Abhishek Banerjee did his Masters in Mechanical Engineering from The University of Texas at Arlington. He earned his Bachelor's degree from the University of Mumbai, India. His research interest is focused on the heat transfer in triangular ducts with H2 boundary conditions and inclusion of axial conduction. He has used Mathematica for all the analytical calculations. His future plan is to gain some industrial experience in the related field and excel in this field. He is a member of American Society of Mechanical Engineers (ASME) and the student education society Tau Beta Pi.